Design of Compact Multi-Path Thomson Scattering Diagnostic with Signal Delay System in Heliotron J*)

Dechuan QIU, Takashi MINAMI[1)], Takuya NISHIDE, Masahiro MIYOSHI, Yuta YAMANAKA, Shinichiro KADO[1)], Shinsuke OHSHIMA[1)], Kazunobu NAGASAKI[1)], Hiroyuki OKADA[1)], Shinji KOBAYASHI[1)], Tohru MIZUUCHI[1)], Shigeru KONOSHIMA[1)] and Ryo YASUHARA[2)]

Graduate School of Energy Science, Kyoto University, Gokasho, Uji, Kyoto 611-0011, Japan
[1)]*Institute of Advanced Energy, Kyoto University, Gokasho, Uji, Kyoto 611-0011, Japan*
[2)]*National Institute for Fusion Science, 322-6 Oroshi-cho, Toki, Gifu 509-5292, Japan*

(Received 6 January 2020 / Accepted 18 May 2020)

A new design of a multi-path Thomson scattering system with signal delay function based on a polarization control technique is proposed on Heliotron J to deal with the overlapping phenomenon of scattered light signals. By operating double Pockels cells to control the injection timing of the laser beam into plasma, the adjacent scattering signals corresponding to opposite incident laser beams are expected to be separated to some extent for better analyzing the anisotropic temperature. Two image relay systems are also designed and integrated into the system to suppress the reduction of the laser beam power during multi-path propagation. Estimations are made on residual power of laser and separation degree of adjacent scattered light signals to reveal the feasibility of this new design. This design is instructive for fusion devices that desire anisotropic measurement but also face limitations of less setting optical path.

Keywords: multi-path Thomson scattering, anisotropic velocity distribution, Pockels cell

DOI: 10.1585/pfr.15.2401044

1. Introduction

Anisotropic measurement is important for understanding the mechanism such as electron cyclotron current drive in toroidal devices [1]. By obtaining the electron velocity distributions (EVDs) in two different directions, the corresponding electron temperature (T_e) can be deduced [2, 3]. The velocity distribution of the electrons can be obtained by measuring the spectrum of Thomson scattered light. Meanwhile, multi-path Thomson scattering (MPTS) system can produce incident beams injected into plasma with an opposite direction, to realize anisotropic electron temperature measurement.

Recently, a new concept of MPTS based on a polarization technique was proposed, and devices such as GAMMA 10 and LHD have been upgraded [4–6]. This method is based on a polarization technique, so that it can keep the beam in the same optical path with an opposite incident direction injected to plasma several times, which simplifies the calibration compared with, for example, MPTS installed in a TEXTOR system where each laser beam path is different in a concave-mirror-type Thomson scattering system [7].

A compact MPTS is under construction based on single path Thomson scattering installed on Heliotron J to performed anisotropy temperature measurements in plasma [8–10]. However, two adjacent scattering signals overlap with each other because there is a long tail and low decay rate of signal waveforms because of the value of the current-voltage conversion resistance of the pre-amplifier circuit installed in each polychrometer. Although reducing the resistance can increase the decay rate of the wavefront, a degradation of signal-to-noise ratio consequently occurs. Under this circumstance, only a long optical path that provides enough traveling time for the laser beam passing through it can solve the overlapping phenomenon. Unfortunately, there is limited room provided by Heliotron J in the optical path; thus, the length of the optical path used to locate optical components is quite small. This means that the corresponding traveling time of the beam is insufficient, and laser will be injected into plasma again soon. As a result, the scattering signal caused by two adjacent but opposite incident beams will overlap with each other where an analysis cannot be made on an independent scattering signal for obtaining orthogonal EVDs. Therefore, another Pockels cell is proposed to be added into our new system at the short optical path located behind the plasma to confine the beam so that a longer interval between injection timing of laser beams with opposite incident direction can be obtained.

In this study, a new MPTS suitable for compact fusion experimental devices is proposed by utilization of two Pockels cells to realize a signal separation function. Two

author's e-mail: qiu.dechuan.78n@st.kyoto-u.ac.jp
*) This article is based on the presentation at the 28th International Toki Conference on Plasma and Fusion Research (ITC28).

image relay systems are integrated into the optical path to maintain beam quality. Finally, two estimations are made on residual power of laser beam and the separation effect of overlapping signals to demonstrate the feasibility of the new design.

2. Design of Optical Polarization System

As shown in Fig. 1, EVDs in an orthogonal direction can be obtained by opposite incident beams. In this schematic, the going incident beam (GIB) is defined as beam that is going from laser to plasma, whereas the returning incident beam (RIB) is defined as the beam injected into the plasma in the opposite direction compared with that of GIB. k_{gi} and k_{ri} are wave numbers corresponding to GIB and RIB, respectively. k_s is the wave number of scattered light. θ_{bs} and θ_{fs} are the scattering angles between the wave number of scattered light and that of GIB and RIB, respectively. k_{bs} and k_{fs} are wave numbers obtained from vector difference as $k_{bs} = k_s - k_{gi}$ and $k_{fs} = k_s - k_{ri}$ respectively.

For producing laser beams with opposite incident direction as shown in Fig. 1, a new MPTS with double Pockels cells that can realize signal separation to overcome the overlapping phenomenon of scattering signals is proposed on Heliotron J and is shown in Fig. 2. Two optical polarization systems and two image relay systems are the

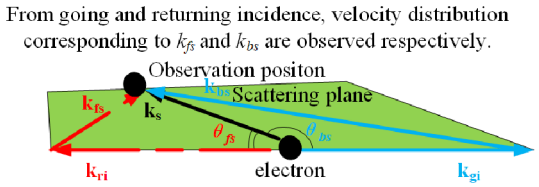

Fig. 1 Schematic view of the scattering configuration with opposite incident beams.

main units of this system. One 50 Hz Nd:YAG laser with a power of ~ 500 mJ and pulse width of 10 ns is chosen as the probe source in the system.

Figure 2 shows a schematic diagram of the new multi-path system with a signal separation function. The beam of a single laser shot can be injected into the plasma several times by the operation of two optical polarization systems enveloped in the dashed line and dashed dot line. The beam in the going incident direction is plotted with a blue line, and its direction points from the left side of plasma to its right. The returning incident direction is plotted in a red dotted line, and its direction is defined from the right of the plasma to its left. Mirror, polarizer, lens, half wave plate, Faraday rotator, and Pockels cell are denoted by M, P, L, HWP, FR, and PC, respectively, with the number after them representing the specific optical component appearing in Fig. 2. Two optical polarization systems are set at both sides of Heliotron J plasma. The 1st optical polarization system is located at the left of Heliotron J plasma whose function reflects the RIB re-inject to plasma. In addition, this system can guide the RIB into a beam dump. The 2nd optical polarization system is located at the right side of the Heliotron J plasma. This system is called the signal delay system (SDS) whose optical path is enveloped in a dashed dot line from M1 to P3 to M2. RIB will be confined in SDS for several reciprocating trips before being released to the plasma. The purpose of guiding the beam into SDS is extending the travel distance of the laser beam. The injection timing of the laser beam corresponding to the returning incidence is postponed in this case so that the scattered light signals caused by the two adjacent incident beams can be separated instead of overlapping with each other anymore. To better distinguish the beam injected into plasma at different timing during a single laser shot, path number N and reciprocating trip number n are introduced.

The beam of one laser shot in a complete optical path in Fig. 2 can be expressed as follows. First, GIB as a linearly polarized beam plotted in blue is guided into the sys-

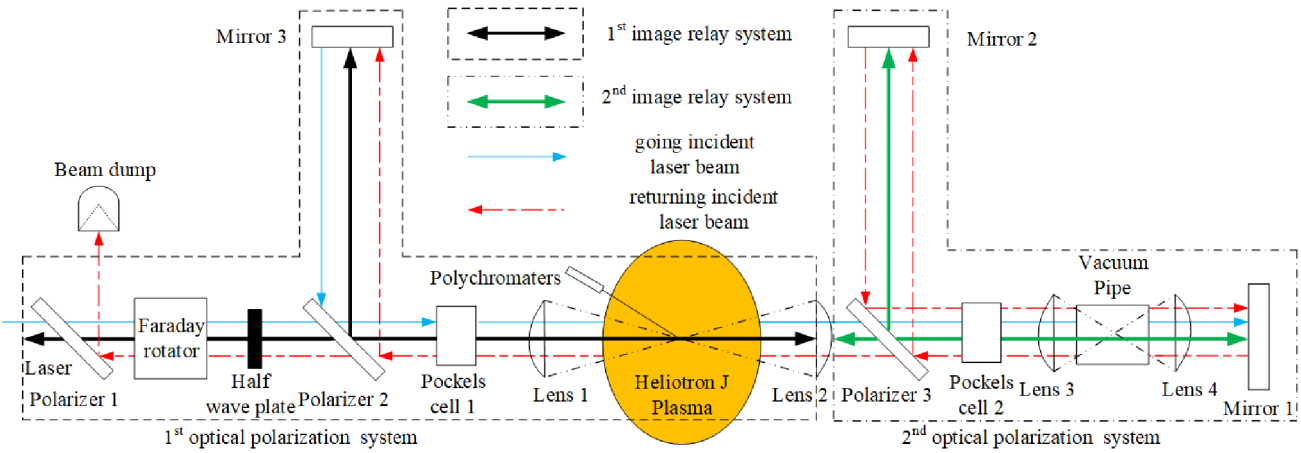

Fig. 2 Schematic diagram of the new multi-path system with signal separation function.

tem from the left side. The beam is plotted in red color when it is reflected by M1 as a returning incident beam. PC2 will be switched on to change the polarization direction of beam by 90° before the entry of the beam. As a result, the beam cannot pass through P3 anymore after its polarization direction changed by PC2 because now its polarization direction is orthogonal to the transmission direction of P3. The beam will be reflected to M2 and will be confined in the optical path of SDS until PC2 is switched off. In this reciprocating trip, n will be increased by 1 every time when the beam reaches M2. PC2 is switched off just before the incidence of beam reflected by M1 to it with n equal to our set of PC2. The beam can be released from SDS and injected to plasma again after PC2 is switched off. In a similar way, the beam will be reflected by P2 to M3 when PC1 is switched on. In contrast, the beam will pass through P3 completely and be guided to the beam dump when PC1 is switched off.

The polarization status of the laser beam can be expressed by Jones matrices, and the Jones matrices of HWP, FR, P, and PC (in operation mode) are expressed as follows

$$P = \begin{bmatrix} 1 & 0 \\ 0 & 0 \end{bmatrix}, \tag{1}$$

$$FR = \begin{bmatrix} \cos\left(-\frac{\pi}{4}\right) & \sin\left(-\frac{\pi}{4}\right) \\ -\sin\left(-\frac{\pi}{4}\right) & \cos\left(-\frac{\pi}{4}\right) \end{bmatrix}, \tag{2}$$

$$HWP = \begin{bmatrix} \frac{1}{\sqrt{2}} & \frac{1}{\sqrt{2}} \\ \frac{1}{\sqrt{2}} & -\frac{1}{\sqrt{2}} \end{bmatrix}, \tag{3}$$

$$PC_{operation\ mode} = \begin{bmatrix} \cos 2\theta & \sin 2\theta \\ \sin 2\theta & -\cos 2\theta \end{bmatrix}, \tag{4}$$

where θ is equal to 45°, and the polarization status of laser light before entry of Polarizer 1 is defined as P0, which is $\begin{bmatrix} 1 \\ 0 \end{bmatrix}$.

The polarization status in a complete travel from P1-M1-P1 can be written as

$$\begin{aligned} &\mathrm{P1 \cdot FR \cdot HWP \cdot P2 \cdot P3} \cdot \prod_{1}^{N} \\ &\cdot \left[\mathrm{P3 \cdot PC1 \cdot PC1 \cdot P3} \cdot \prod_{1}^{n} (\mathrm{PC2 \cdot PC2 \cdot}) \right] \\ &\cdot \mathrm{P3 \cdot P2 \cdot HWP \cdot FR \cdot P1 \cdot P0} = \begin{bmatrix} 0 \\ 0 \end{bmatrix}. \end{aligned} \tag{5}$$

The outcome is $\begin{bmatrix} 0 \\ 0 \end{bmatrix}$ which means the beam is reflected to the beam dump and nothing passes through P1 anymore.

To calculate the signal separation efficiency of our design, the delay time τ can be calculated as

$$\tau = (2 \times D_{L2toM1} + n \times 2 \times D_{M1toM2})/c, \tag{6}$$

where D_{L2toM1} and D_{M1toM2} are the distance from L2 to M1 and the distance from M1 to M2 respectively. c is the speed of light and n is the reciprocating number how many times beam travels between M1 and M2 in SDS. D_{L2toM1} and D_{M1toM2} are set as 9.15 m and 9.75 m, respectively, in our design. In this case, the delay time corresponding to n equal to 0, 1, 2, and 3 can be calculated as 61, 126, 191, and 257 ns respectively.

3. Estimated Performance of MPTS with Signal Separation Function

For estimating the performance of the new design, an estimation of the relationship between the residual power of laser beam and path number N with different setting of reciprocating trip number n is shown in Fig. 3. Because a loss occurs when the beam passes through any of the optical components, an assumption is made as the power loss brought by Pockels cell and other optical components are 2% and 1%, respectively, based on the manual provided by the manufacturer. After reaching the plasma, RIB's power has a 15%, 25%, 36% and 45% reduction corresponding to n equal to 0, 1, 2, and 3, compared with the power of previous GIB because it passes at least 7 optical components (n = 0) in SDS. Similarly, a loss of approximately 16% occurs on the power of GIB when it is injected into plasma after the beam passes the components in the 1st optical polarization system.

Figure 3 demonstrates that the residual intensity of laser power decreases as the path number N and reciprocating trip number n increase. The delay time of RIB can be prolonged with the rise of reciprocating trip number n, but the residual power of RIB falls down, which is caused by an increasing number of optical components passed by the beam. Because of the reasons mentioned above, the principle of setting SDS should obey that a certain optical path, and less optical components are better because they lead to a higher residual power of laser beam.

In addition, the separation effect of SDS on overlap of adjacent scattered light signals is investigated. Because

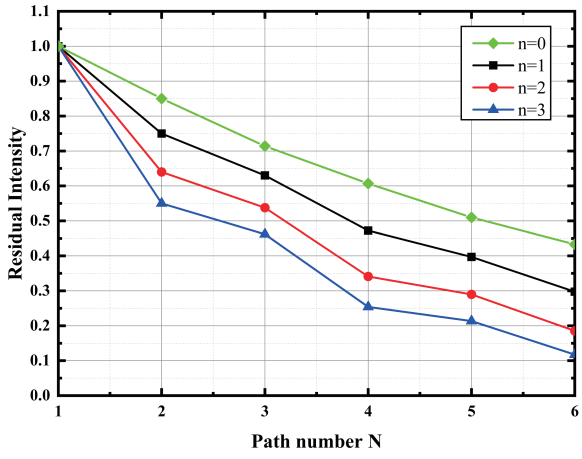

Fig. 3 Relationship between intensity of laser power and path number N with different reciprocating trip n.

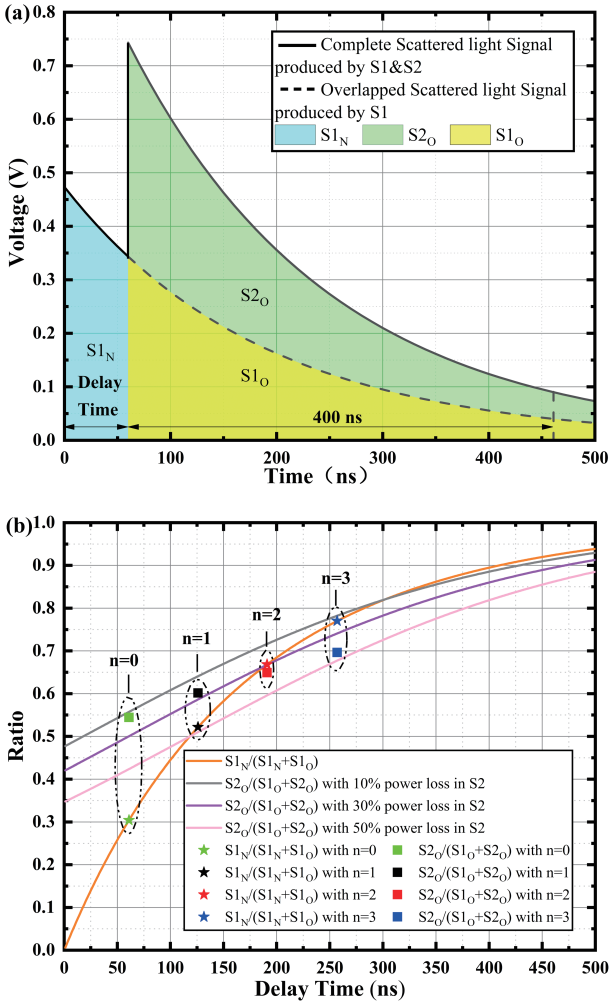

Fig. 4 (a) Typical overlap between two adjacent scattered light signals. (b) Ratio between overlap and non-overlap integration part with different delay time.

the scattered light signal is considerably close to each other when delay time is insufficient, the non-overlapped part of a pure signal is limited to deduce anisotropic data. Thus, only by separating overlapped signals sufficiently can we achieve more scattered light signal belonging to one incident beam. The overlap on adjacent scattered light signals is shown in Fig. 4 (a) to demonstrate two ratios as reference parameter of the separation effect. The response signal of avalanche photodiodes (APD) is utilized to simulate the actual scattered light signal. The response signal of APD is evaluated as an exponential function and its decay time is around 200 ns, based on an experimental data of our previous work [10]. S1 and S2 correspond to the signal produced by GIB and RIB respectively. The acquisition time is defined as the sum of delay time and 400 ns. The 400ns starts from the appearance of S2. The non-overlapped part of S1, overlapped part of S1 and S2 are expressed by $S1_N$, $S1_O$ and $S2_O$, respectively. Since the short time interval between the timings of GIB and NIB, S2 is completely overlapped with S1. Blue area, yellow area and green area correspond to the time integration of $S1_N$, $S1_O$ and $S2_O$ respectively. In this case, $S1_N/(S1_N+S1_O)$ is the ratio that reflects the percentage occupied by non-overlapped S1 in the complete S1. The higher $S1_N/(S1_N+S1_O)$ is, the more signal we can achieve from $S1_N$ to deduce the anisotropic data relating to GIB. In contrast, $S2_O/(S1_O+S2_O)$ represents the ratio that reflects the percentage occupied by S2 in the overlapped signal that is the sum of $S1_O$ and $S2_O$. The higher $S2_O/(S1_O+S2_O)$ is, the more convincing we can take the sum of $S1_O$ and $S2_O$ as the pure signal produced by RIB, which means the anisotropic data relating to RIB deduced from the overlapped part becomes more reliable.

Based on the above definitions, the trends of the ratios $S1_N/(S1_N+S1_O)$ and $S2_O/(S1_O+S2_O)$ over different delay time are shown in Fig. 4 (b), to demonstrate how much ratio is sufficient for separating two adjacent signals. The orange line is the trend of $S1_N/(S1_N+S1_O)$ to delay time. The grey line, purple line, and pink line are the trends of $S2_O/(S1_O+S2_O)$ to delay time with power loss in the S2, which are 10%, 30%, and 50%. The star and square in green, black, red and blue correspond to the double path situation shown in Fig. 3 with different set of n. If the power loss on S2 isn't higher than 50%, it can be seen that both ratios are higher than 0.5 when the delay time exceeds 120 ns, which means both proportion of $S1_N$ in S1 and proportion of $S2_O$ in the sum of S1 and S2 account more than half.

Because the typical signal to noise ratio (SNR) greater than 2 in our single path system, meanwhile if both the ratios shown in Fig. 4 (b) are over 0.5, the SNR of MPTS can be over 1. In this case, it is possible to separate two adjacent scattered signals by fitting the $S1_N$ as exponential function. Specifically, by operating the SDS, the value of $S1_N/(S1_N+S1_O)$ rises up to 0.52, 0.67 and 0.78 when the delay is 126, 191, and 257 ns, respectively. For $S2_O/(S1_O+S2_O)$, its value increases from 0.55 to 0.6 by 10% at least with the shortest delay time as 126 ns.

In summary, for the double path of our design, the condition in which these two ratios higher than 0.5 can be achieved only by applying SDS.

4. Summary

In this study, a MPTS system is designed with signal delay system, which comprises two optical polarization systems and two image relay systems. By operating the SDS, two overlapped scattered light signals are efficiently separated so that EVDs belonging to two different directions can be achieved. In addition, this design is instructive for fusion devices that desire anisotropic measurement but also face limited room for setting optical path. For the future anisotropic measurement on Heliotron J, this design will be implemented based on the minimum delay time estimated above.

Acknowledgments

The authors are grateful to Heliotron J staff for conducting the experiment. This work was supported by the Collaboration Program of the Laboratory for Complex Energy Processes, IAE, Kyoto University, the NIFS collaborative Research Program (NIFS10KUHL030, NIFS17-KUHL074, NIFS17KUHL076, NIFS18KUHL083, NIFS18KUHL085, NIFS16KOAH035, NIFS18KLEH071), JSPS KAKENHI Grant Number JP19K03792 and "PLADyS" JSPS Core-to-Core Program, A. Advanced Research Networks.

[1] K. Nagasaki *et al*., Nucl. Fusion **47**(8), 1045 (2007).
[2] E. Yatsuka *et al*., Nucl. Fusion **51**, 123004 (2011).
[3] T. Matoba *et al*., Jpn. J. Appl. Phys. **18**, 1127 (1979).
[4] R. Yasuhara *et al*., Rev. Sci. Instrum. **83**, 10E326 (2012).
[5] M. Yoshikawa *et al*., Rev. Sci. Instrum. **83**, 10E333 (2012).
[6] I. Yamada *et al*., Rev. Sci. Instrum. **83**, 10E340 (2012).
[7] M. Yu Kantor *et al*., Plasma Phys. Control. Fusion **51**, 055002 (2009).
[8] N. Kenmochi *et al*., Plasma Phys. Control. Fusion **59**, 055013 (2017).
[9] T. Minami *et al*., to be submitted to JINST (2019).
[10] N. Kenmochi *et al*., Rev. Sci. Instrum. **85**, 11D819 (2014).